OTC-27815-MS

Pipe-Clamping Mattress to Stop Flowline Walking

Sebastiaan Frankenmolen and Sze-Yu Ang, Shell Global Solutions; Ralf Peek, Peek Solutions; Malcolm Carr and Ian MacRae, Crondall Energy; David White, University of Western Australia; Jeffrey Rimmer, Shell Philippines Exploration and Production

This paper was prepared for presentation at the Offshore Technology Conference held in Houston, Texas, USA, 1–4 May 2017.

Abstract

Thermal gradients from a heating front travelling down a flowline at start-up can cause a flowline to walk much like a worm creeps by repeated contractions and expansions of its body. To stop this for the Malampaya flowline, pipe-clamping mattresses (PCMs) were invented, developed, and deployed within a period of 12 months. The objective of this paper is to share the knowledge and experience from this novel but effective solution to mitigate pipeline walking.

PCMs provide a cost-effective alternative to rockdump or conventional mattresses to axially restrain a pipeline at a location chosen so that the required restraint capacity is minimized. They are inspired by conventional mattresses and bear some similarity to them, but they are designed so that the weight of the mattress acts to clamp the pipeline with a high leverage. Thus 100% of the weight of the mattress is effective in generating axial friction with the seabed. This solution can be applied at any point along the line (chosen to minimize the required resistance) without requiring flanges or collars on the pipeline.

From the most recent survey results 15 PCMs with a dry weight of around 9 tons per PCM, plus 7 tons for the logmat installed over every PCM appear to be effective to stop the walking of the Malampaya flowline. This performance is as expected from extensive analysis (FE and otherwise) to reproduce the observed walking behavior prior to restraining, to estimate the required restraint capacity, and to estimate the resistance provided by the PCMs.

This paper describes the PCM, the clamping forces they generate by leveraging the weight of the PCM and logmats installed over them, and how the friction generated with the soil is estimated from interface shear tests on samples collected from the site, considering cyclic pore pressure generation and dissipation effects. It also briefly covers FE analyses to reproduce the observed walking behavior, and determine the required restraint capacity, the PCM fabrication, installation, and monitoring of the post-installation performance.

Introduction

Pipelines and flowlines can walk or creep, a bit like a worm does by axial contractions and expansions of its body. This phenomenon has become well-known [Konuk (1998), Tornes et al. (2000), Peek (2002), Carr et al. (2006), Bruton et al. (2010), Carneiro et al. (2014)]. Restraints to prevent walking can be large and expensive. They are often installed because finite element (FE) simulations indicate the flowline could

walk, if not restrained. Walking was less well known around 1996-97, when the twin 16-inch diameter Malampaya flowlines were designed. The flowlines carry multi-phase gas with some condensate from the Malampaya and Camago fields in around 800m water depth, over 28.3km to a platform in about 40m water depth. The condensate is then separated from the gas and stored for periodic off-loading to tankers, and the gas is taken via the 500km-long Gas Export Pipeline to Batangas, near Manila, on the Isle of Luzón, where it covers about 30% of the power demand on the island. No special provisions were made at the design stage to prevent walking. Walking did occur, however, with about 28mm displacement per shut-down and restart cycle, which had accumulated to a displacement of 1.8m, at the Pipeline End Structure (PLES). This started raising concerns over the integrity of the jumper connection from the PLES to the manifold, where the production from 11 wells is collected and distributed over the two flowlines. (Only one of the two Flowlines experienced significant amount of walking. The other was not in use for much of the time.)

This paper first describes the walking phenomena as observed for the flowline, including the interactions with lateral buckles, and the finite element simulations of them. Then it describes a novel way of restraining such walking, by use of pipe-clamping mattresses (PCMs). It describes circumstances and considerations leading to inventing the PCMs, their design, fabrication, trials, and deployment, all completed within a period of less than 12 months. Finally, performance monitoring results since the time of installation in December of 2015 are also included. A patent application has been filed for the PCMs.

Description of the Walking Behavior and FE Simulations Thereof

Walking is caused by cyclic expansions and contractions of the pipeline, together with a mechanism that makes the movement at each cycle in one direction a bit more than in the other. In this case, the contraction at the inlet upon cooling each time the line is shut down is a bit more than the expansion displacement upon restart. Most recently (before the remediation by the PCMs) the difference was about 28mm. Over almost 200 cycles, this had lead a total displacement of the inlet of about 1.8m in the downstream direction (this is in the opposite direction to the natural expansion of the pipeline, which was anticipated to be about 2m in the upstream direction). Evidence of walking could be seen from marks in the seabed left by pile guides on the PLES (see Figure 1) and was further monitored by flags, as shown in Figure 1.

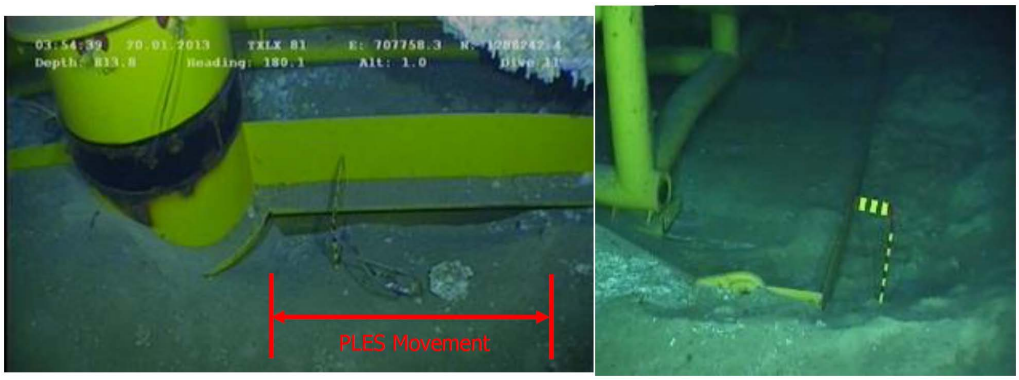

Figure 1—Evidence of Movement of the PLES at the inlet of the flowline, and flags used to measure displacements

The PLES includes an upper moving part with flowline and spoolpiece connection and a lower part resting on the seabed. the upper part can slide on rails on the lower part, so that the usual thermal expansions and contractions can be accommodated without the PLES sliding over the seabed each time. However, the walking made the slider bear hard against its end, upon contraction. Thus, the flowline started to pull the entire PLES with it, resulting in the displacements shown in Figure 1.

In this case the main driver of walking are thermal gradients. The worst-conceivable thermal gradients involve a heating front travelling down the line upon start-up [Peek (2002)]. Thermal gradients can be

shown to be equivalent to applying an axial force proportional to the thermal gradient acting in the direction of decreasing temperature. Typically, the start-up fronts create thermal gradients travelling down the line that are much larger than those at steady-state operations. To capture this, it is essential to first perform multiphase flow simulations of the start-up process, in order to obtain the correct inputs to the FE analysis for temperature, pressure, and density of contents as a function of time t and location x along the flowline.

Matters are further complicated by the bathymetry and liquid accumulation: The inlet is at a low point. This means that gravity tends to drive walking in the opposite direction to that in which it occurred, i.e. in the upstream instead of downstream direction. Both FE simulations and observations at the PLES indicate that walking in the upstream direction is indeed what happens in the first few cycles (see Figure 5), but after about 50 cycles, the walking changes direction, heading downstream, apparently driven more strongly by the thermal gradients (acting in the downstream direction), than by the gravity (acting in the upstream direction). Gravity loads are not the only effect of the bathymetry, however. It also causes accumulation of liquids at the inlet upon shut-down. Upon start-up, this large slug is pushed down the line. This influences the thermal gradients. Also, the associated changes in weight influence the axial pipe-seabed interaction, with significant impact on the walking behavior.

The walking pipeline must go somewhere. For a short flowline, the entire length can walk. However, for the 28.3km-long Malampaya flowline, the walking feeds mostly into lateral buckles. The first one occurs at around KP 1 (i.e. 1km from the inlet), and a total of 8 buckles are observed with the last one 8km from the inlet. The spacing between lateral buckles ranges from 0.5 km to 1.5 km. The first buckle occurs at a local high point that acts as a trigger. That buckle has also developed very large lateral displacements (~14 m) together with a very large wavelength of 400m. (Here the "wavelength" means the length of the pipe over which it is laterally displaced.) FE simulation revealed that the bathymetry not only triggered the first buckle, but also creates a lateral walking mechanism as follows: when the pipe goes into compression due to the temperature rise, the vertical curvature makes it lift off the seabed, or, at least, it reduces the lateral friction that can be generated with the seabed, thus reducing the resistance to lateral movement. However, when the pipe cools, it goes from compression into tension. This tension, acting through the curvature associated with the bathymetry, causes the pipe to dig downward into the soil at the apex of the buckle. The result is that the apex is restrained from pulling back laterally upon cooling. Instead the pipe gains greater straightness by additional outward lateral displacements away from the apex of the buckle. Then when the pipe heats up again, it starts from this outward position, and develops larger lateral displacements at the apex than at the previous cycle. Ultimately this results in the very large lateral displacement over a very long wavelength. The mechanism is illustrated in Figure 2.

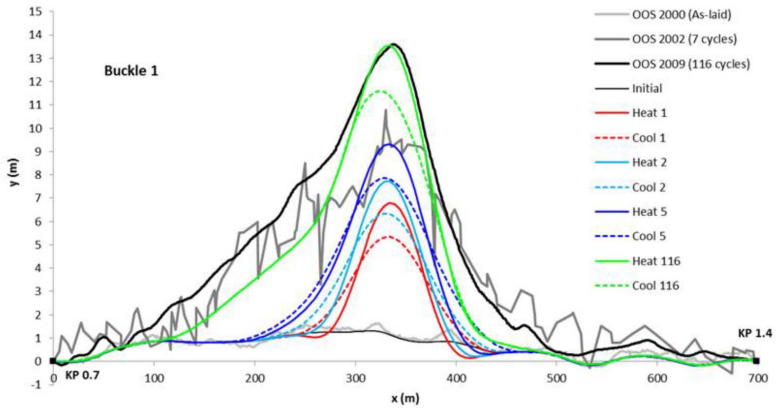

Figure 2—Growth of buckle at KP1.0 (Curves labelled "Heat" or "Cool" are from FE analyses, after the stated number of cycles, whereas those labelled "OOS" correspond to the ROV survey performed in the year shown. The OOS 2000 trace shows the position of the pipeline prior to operation. The corresponding number of cycles are about 7 for the year 2002, and 116 for the year 2009.)

Indeed, the FE simulations showed that, without the formation of huge berms (such as the one shown in Figure 3), the lateral walking simply continues to pull more and more pipe into the buckle.

Figure 3—Trench and berms created by the sweeping action of the pipeline at the first lateral buckle

To simulate these and other features of the behavior, the FE model, constructed with Abaqus, has the following features:

- The pipe is modeled with "pipe" elements in Abaqus, which are essentially beam-type elements, but also account for internal and external pressure, and the effect that the associated hoop stress has in the stress-strain relation in the axial direction. The model covers the first 15 km of the pipeline within which all of the lateral buckles form. The length of the model is sufficient to capture the axial feed-in for the last buckle.
- It accounts for material and geometric non-linearity, including a frictional model for pipe-soil interaction with different friction coefficients in the axial and lateral directions. The best fit to the "observed" buckling and walking behavior was obtained with a friction coefficient of 1.0 for both the axial and lateral directions, together with an uncoupled model in which the axial resistance depends only on the axial displacements and the lateral resistance depends only on the lateral displacement, though both are frictional and thus depend also on the vertical component of force between the seabed and the pipe. Subsequent additional geotechnical data collection and special soil-pipe interface shear tests conducted at Fugro AG in Perth led to a median estimate of the axial resistance after full consolidation of 0.94 times the weight of the pipe, which is excellent agreement with the axial friction factor from the matching exercise.
- The formation of berms and trenches as shown in Figure 3 is modeled approximately by lateral springs that are created and removed repeatedly as judged appropriate, with resistances chosen to match the surveyed buckle amplitudes, and, if necessary increased as a function of cycle number to whatever it takes to reduce the lateral walking to the measured levels of lateral displacement.
- Changes in temperature, pressure and contents density as function of KP location x and time t are accounted for. These parameters are obtained by bilinear interpolation between a grid of points (x,t) for which the results of the multiphase flow start-up and shut down simulation (calculated with Olga) were transferred as input to the FE simulation. For this it is important to use a sufficiently fine grid of points (x,t), and especially small increments in time (t) initially. Also, sufficient mesh refinement is needed for the Olga model to capture the rather sharp start-up transients.
- It accounts for bathymetric changes along the line, but bathymetric changes in the direction normal to the pipeline route are neglected, by assuming the seabed is flat in that direction.
- As-laid geometry is captured by forcing an initially straight pipe into the surveyed shape, and then releasing it onto the seabed. Upon release, this FE simulation smooths the survey data, providing

the starting point for hydrotest and operational loads to be applied. During the initial forcing and release, the pipe is assumed to remain elastic. (Otherwise unrealistic plastic deformations associated with short wavelength errors in the survey data would occur during the forcing. After release, the stresses were within the yield stress of the pipe everywhere). With this modeling of the lateral and vertical out of straightness, most FE model buckles formed at the observed locations. Where this was not the case, lateral loads were applied in a subsequent analysis to trigger the buckles at the correct locations and in the correct direction. These artificial triggering loads are reduced back to zero before the operating temperature and pressure are reached, and are applied only at the start of the first heating cycle only, and not for subsequent cycles.

A limited number of sensitivity analyses, varying inputs to the FE and Olga models within their range of uncertainty produced considerable changes in the results. Therefore, a matching process was applied, to arrive at the results that best matched the survey data. The matched model was then used in subsequent analyses to determine the restraint capacity required to stop the walking. This matching process produced a reasonable match for both the lateral buckling displacements (Figure 4) as well as for the walking displacements at the PLES (Figure 5).

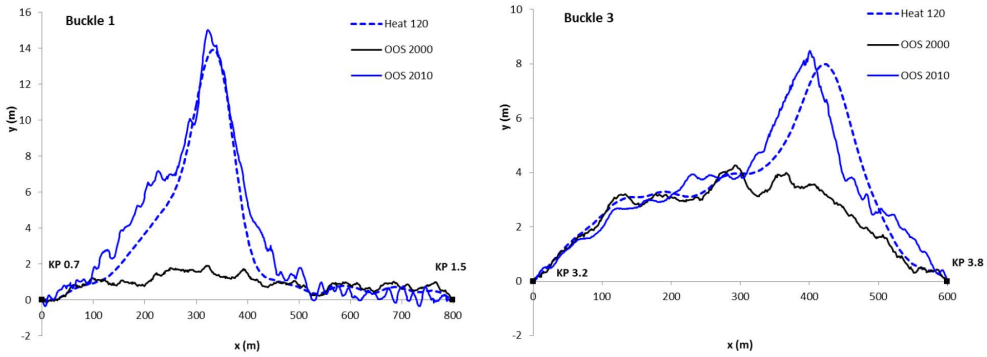

Figure 4—Lateral buckling profiles from surveys and FE simulation for buckles at KP1.0 and KP3.6 (Curves labelled with "OOS" followed by the year are from ROV surveys; those labelled by "Heat" followed by the cycle number are from FE analysis. The "Heat 120" results correspond to the number of cycles which occurred prior to the 2010 OOS survey.)

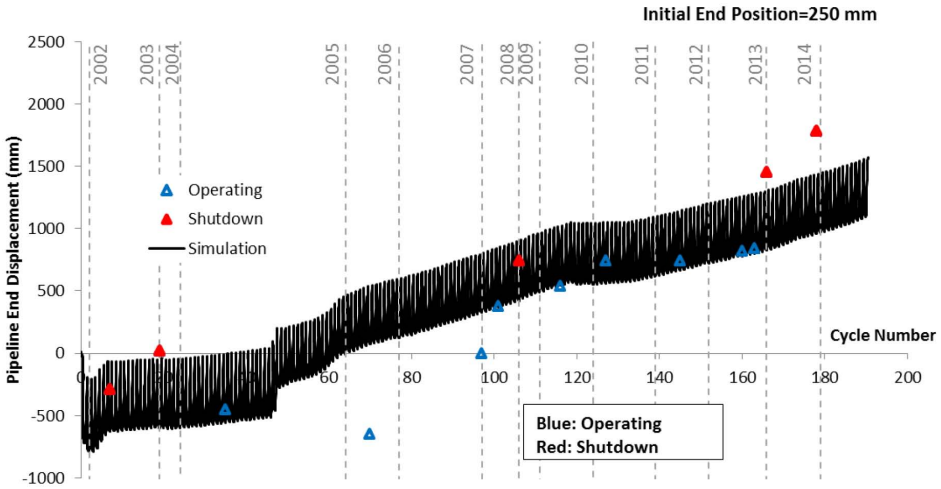

Figure 5—History of axial displacements at the PLES as a function of cycle number, from observations as in Figure 1 and from FE simulation.

This matching process was not based on formal optimization. Instead it relied largely on engineering judgment to select suitable inputs, guided by results of earlier runs.

One of the matching challenges arose as FE simulations did not readily carry the walking displacements to feed the more downstream buckles as appeared to be the case from the survey data. This was improved by sharpening the temperature fronts. I.e. instead of using the Olga outputs directly in the FE simulation, the histories were modified slightly to create sharper fronts, as might be produced by the slug of liquid being pushed away from the inlet in a way that may not have been accurately captured in the Olga simulations.

Optimum Location of Restraint and Estimation of Force Acting on it

The optimum restraint location is the location where walking can be stopped with the minimum required load carrying capacity of the restraint. This is not at the PLES where large cyclic displacements occur, but further downstream, about two thirds of the way to the first buckle. To find this optimum location, the cyclic axial displacements from the FE analysis without the restraint were considered (Figure 6). The location where this cyclic displacement is smallest was selected as the optimum restraint location, and this was confirmed by additional analyses including a restraint at different locations and calculating the forces generated at the restraints. A combination of sensitivity analysis, and engineering judgment considering the uncertainties in the various inputs to the FE simulations was used to estimate the probability distribution for the maximum force on the restraint shown in Figure 7. It then remains to create a restraint with this required capacity at that location.

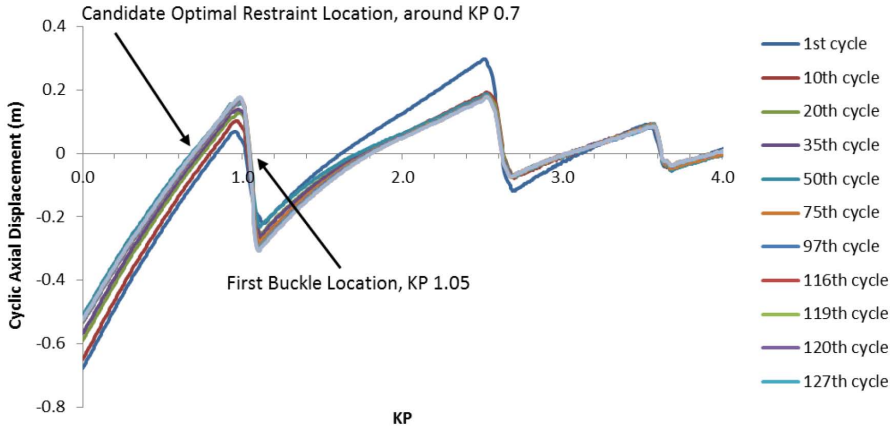

Figure 6—Cyclic axial displacements, defined as the change in axial displacement upon start-up from cold to steady-state operating conditions.

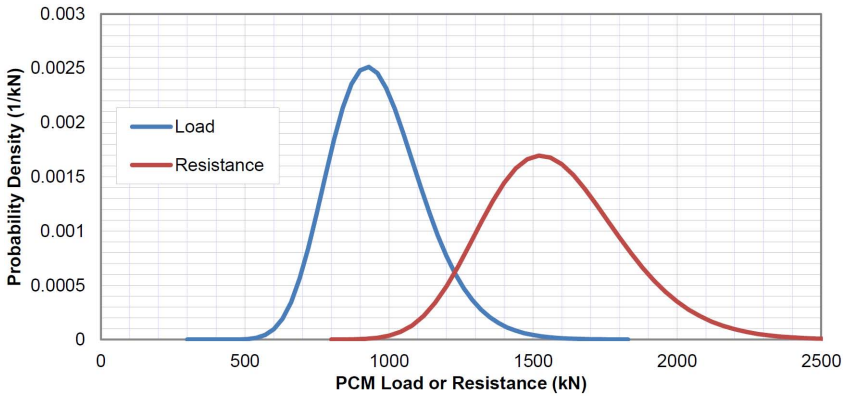

Figure 7—Estimated probability distribution for the force acting on- and the resistance of the restraint to stop the walking. The resistance is based on 15 PCMs reaching fully consolidated (i.e. drained) conditions.

The PCM Concept and Load Capacity of PCMs

One way to restrain the pipe axially is to place rock dump on it. The amount of rock needed to generate the required restraint capacity is not large, but mobilizing a suitable vessel capable of accurately placing the rock in 800m water depth to the Philippines is expensive.

As an alternative, ordinary concrete mattresses placed over the pipe were considered. Simple and FE analyses indicated that such mattresses were effective if some membrane tension in the mattress across the pipe were maintained. However, if the pipe works itself deeper into the soil, the mattress could go from membrane tension to compression, essentially arching over the pipe. In this event, the standard mattress provides very little axial restraint, if any at all. Improved mattress concepts which could improve the wedging action were also considered, but also suffered the drawback that they tend to push the pipe down deeper into rather soft soil, and become ineffective.

These considerations together with an increasing urgency to come up with a solution finally lead to the invention of the Pipe-Clamping Mattress (PCM). Instead of simply resting on the pipe, the PCM (Figure 8) clamps the pipe into it, using its weight at a high leverage. Indeed, the PCMs are designed so that the clamping capacity between the PCM and the pipe overmatches the sliding capacity of the PCM with the pipe over the soil. Thus 100% of the weight of the PCMs is effective in generating axial frictional resistance. A log mattress is provided over every PCM to provide additional weight and especially additional clamping force. The log mattress is more efficient in generating clamping force, because its weight is delivered to the outer extremities of the PCM, whereby leverage is maximized.

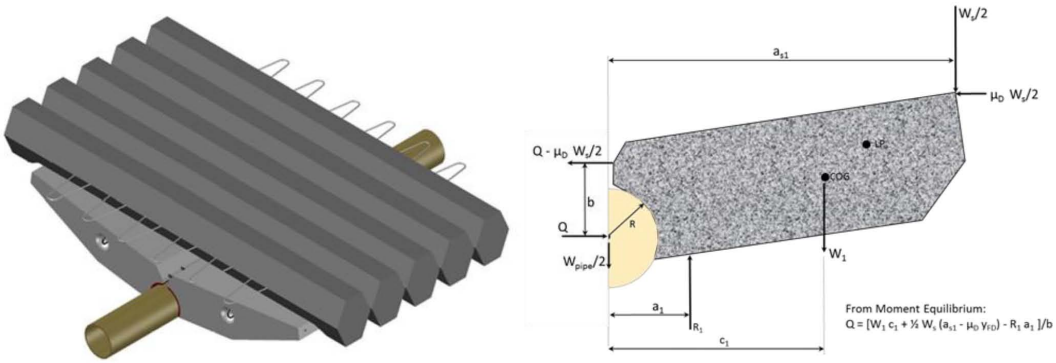

Figure 8—(a) Pipe-Clamping Mattress (PCM) with logmat. (b) Equilibrium considerations to determine the PCM clamping force Q

Simple equilibrium calculations (Figure 8) were found to give accurate estimates of the clamping force generated and the axial capacity against sliding between the PCM and the pipe, when compared to 2-dimensional FE analyses in which the soil is modeled as an elasto-plastic continuum. These FE models employ a slice of elements normal to the pipe, with boundary conditions set in such a way that both plane strain and antiplane shear deformations are captured. This was achieved by making the displacements of corresponding nodes at each side of the slice the same.

Of course, the stresses in the pipe due to clamping by the PCM were calculated. They are well within the allowable limits even if the clamping force were concentrated as line loads at the 3 and 9 o'clock positions. Also, the effect of the shear and normal forces on the coating had to be considered, together with the effect of temperature on the 3-layer-PP coating strength, and concentrations in the PCM-pipe contact stresses due to geometric variability within specified tolerances.

Geotechnical Aspects

An essential requirement for the development of a suitable restraint system is adequate understanding of flowline-soil and mattress-soil interaction for representative loading conditions. Time- and loading-dependent friction factors between the mattresses and the seabed and the pipe and the seabed were key items required to quantify the weight and number of PCMs, and to verify the modelling of the history of expansion and buckling. Initially, no geotechnical data were available for the proposed restraint location. The seabed at the proposed PCM location was expected to comprise very soft soil.

Site specific geotechnical data were acquired to develop reliable site-specific geotechnical parameters for the development of the restraint. Notwithstanding the challenging constraints of limited time and budget, the geotechnical SI was conducted in September 2014 and high quality samples were successfully recovered by piston corers. Based on standard laboratory tests, the seabed was classified as siliceous CARBONATE SILT in accordance with the classification systems proposed by Clark and Walker (1977). It is reasonably uniform and laterally homogenous within the proposed PCM location.

To develop the time-dependent soil resistance to cyclic axial pipe movements, monotonic and cyclic interface shear tests were also performed. These tests are similar to direct shear tests on soil only, but instead of creating a shear plane within the soil, they create a shear plane at the interface between the soil and a surface with the same roughness as the coating of the pipe. The general arrangement of this apparatus and a post-test view of a sample are shown in Figure 9. These tests aim to reproduce the loading history at the pipe-soil interface, including generation and dissipation of pore pressures. They were performed in Fugro AG's Perth laboratory using a direct shear apparatus incorporating modifications to suit testing with the low stress levels and episodic movements representative of pipelines. These modifications include a lightweight hangar, a low friction carriage, and careful calibration of corrections for machine friction before each test series.

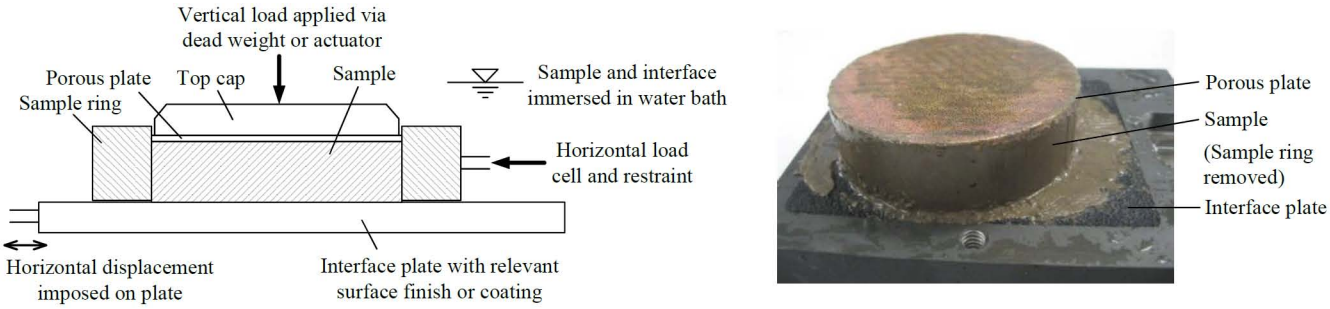

Figure 9—(a) Interface shear box apparatus (b) View of sample after completion of test and removal from apparatus (White et al. 2012)

Thus the following effects could be captured using the approach described in White et al. (2015), and in Atkins (2015): (i) the effect of stress level on drained interface friction angle; (ii) the effect of loading rate on interface strength for normally consolidated soil and overconsolidated soil; (iii) the effect of over-consolidation on undrained interface properties and (iv) the cyclic hardening (or softening) behavior of the interface through cycles of undrained shearing and consolidation. The cyclic hardening, through episodes of undrained movement followed by consolidation (pore pressure dissipation) prior to a subsequent movement, is the process that occurs during the operating life of the flowline, and leads to a change in the interface strength.

Figure 10 shows an example result from the interface shear box test program. The sample was initially consolidated to an effective stress of 25 kPa. Then two cycles of +/- 9 mm shear displacements were applied at a rate of ~1 mm/s to ensure essentially undrained shearing. This is followed by a 30-minute dissipation period. The sequence of undrained shearing followed by dissipation is then repeated. The resulting shear

stress vs. shear displacement relations from such a test are shown in Figure 10. The steady or residual interface shear strength rose from 0.45 times the total vertical stress in the initial cycle pair to about 0.8 times the vertical stress in the final cycle. The initial value represents the normally-consolidated undrained interface strength ratio, R_{int} (which can be denoted $(s_{u\text{-}int}/\sigma'_{no})_{nc}$), and the final value represents the drained strength, $\tan(\delta_{res})$, corresponding to this stress level (and the particular interface material and roughness used). The plot also shows that this final value is already reached for shearing cycles 11 & 12, which take place after 5 cycles of dissipation. The shearing in this case represents a shut-down/restart sequence, which could be of short duration (of around 1 day), whereas the dissipation cycle represents the longer period (of around 1 month) of operating at approximately steady-state conditions.

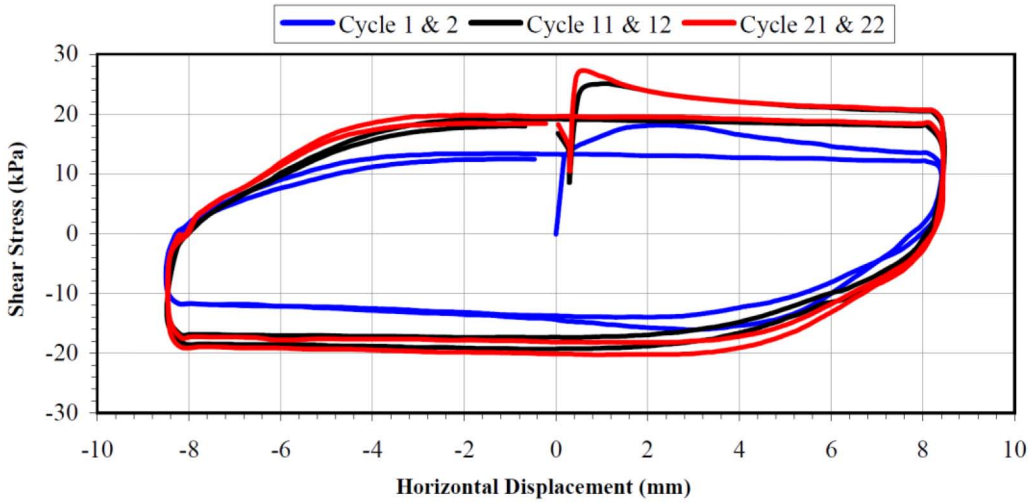

Figure 10—Typical results of episodic interface direct shear test, with 30min of dissipation at an effective stress of σ'_{no}= 25 kPa initially and after every pair of essentially undrained dissipation cycles.

This pattern of cyclic hardening is consistent with previous reported studies but the specific values of the soil parameters – including the high values of R_{int} and δ_{res} – are different from typical values for non-carbonate clays and reflect the carbonate mineralogy of the seabed sediment in the Malampaya region. The site-specific sampling and testing was therefore valuable in identifying the interface strength parameters relevant for this site.

A further important parameter for the geotechnical analysis is the coefficient of consolidation, c_v, at near-surface depths of a few tens of centimeters. This parameter is important since it controls the time required for dissipation of any generated excess pore pressures and the associated changes in effective stress and undrained strength beneath the pipeline and mattress after installation and following any undrained movements. Near-surface measurements of c_v are difficult to obtain using conventional in situ tests such as the cone penetrometer dissipations. The design range of c_v was estimated based on the consolidation stage of the interface shear box tests supported by extrapolation of the trend from deeper measurements.

The same interface shear tests also served to estimate the sliding resistance between the PCMs and the soil. This was supplemented by a few extra tests in view of the higher roughness of the PCM surface, as opposed to the PP-coated pipe. The assessment indicated that the PCMs are initially supported mostly by the pore water trapped in the soil, which provides very little resistance to sliding. A dissipation time of about one month was estimated for these pore pressures, based on the consolidation times for the interface shear tests, and scaling this to account for the longer drainage paths for pore water trapped under the PCMs, as opposed to that in the much smaller interface shear tests. (The PCMs have holes covered with geotextile to enable quicker dissipation of pore pressures.)

Upon first consolidation, under the weight of the PCMs alone, the PCM sliding resistance already increases significantly. It increases even more after several cycles of shearing and re-dissipation of the excess pore pressures generated by each shearing event, until finally the drained sliding resistance applies (even for undrained movements), after about 5 cycles of dissipation or more. Since 5 cycles of walking could be tolerated, the design was based on this drained sliding resistance. The estimated probability distribution for the drained sliding resistance is shown in Figure 7, together with the probability distribution of the load acting on the restraint. Other results from the geotechnical assessment include: flowline force-embedment relationship applicable during installation (undrained conditions), short- and long-term embedment of the PCMs, and mobilization displacement for the load-displacement relation associated with sliding of the PCM over the seabed. In all cases, low, median, and high estimates were made.

The offshore trials provided a rare (if unplanned) opportunity to confirm low initial resistance to sliding. For this, a friction coefficient of less than 0.05 was estimated when the PCM or pipe is initially placed, and mostly supported by pore pressures from water trapped in the soil below. A joint of pipe was lowered to the seabed at a location which had a slope of approximately 1 in 12. The pipe joint was observed to slide away axially as the supporting sling went slack, indicating an interface friction coefficient of < 0.08. Fortunately, no axial resistance was needed from the PCMs so early on. Nevertheless, this illustrates an important point about pipeline on soft, normally-consolidated seabeds. Before sufficient time has elapsed for the pore pressures from the pipe weight to dissipate, the available axial friction coefficient is very low. This may have implications for pipeline stability when laying around curves or on slopes.

Structural Reliability Assessment (SRA)

In lieu of an established design procedure for restraints intended to stop walking, structural reliability assessment (SRA) was used to define the safety margins required to cover the uncertainties involved. For this purpose, all relevant uncertainties were estimated explicitly and combined to calculate the failure probability. The number of PCMs was then chosen to keep this failure probability below a tolerated level. Here a simplified, approximate approach was used, so that a few sensitivity analyses with the FE model were sufficient, instead of having to incorporate the FE model within one of the algorithms used for calculation of failure probabilities, such as first or second order reliability calculations, Monte-Carlo simulation, or other method.

All identified and relevant uncertainties were included, even if, in lieu of statistical data, the estimates of the probability distributions had to be mainly based on engineering judgment. The SRA involves a load side and a resistance side for the PLES displacement.

On the resistance side, the probability distribution for the PLES displacement at which the connecting spoolpiece fails is estimated using an FE model of the spoolpiece. This FE model leads to the bending and torsional moments at the spool-piece-to-PLES connector, which is the potential weak link. Uncertainties considered for this include: the moment capacity of the connector, the initial position of the sliding part of the PLES on its base, the initial stresses in the spoolpiece at the time it is connected (arising for instance when the connector pulls the connection together), the friction factor between the spoolpiece and the seabed, the settlement of the PLES and the associated increase in the frictional resistance between the spoolpiece and the pipe, and eccentricity of soil resistance to sliding of the PLES, which would in part be resisted by bending moments in the spoolpiece that prevents the PLES from rotating about a vertical axis. (The yield strength of the spool piece was not judged relevant, since the most likely failure scenario involves loss of integrity of the connector before any yielding of spoolpiece. Thus, the one uncertainty for which statistical data are available was not relevant in this case.)

On the load side, the additional displacement that might develop before the soil is sufficiently consolidated for the PCMs to stop the walking was estimated considering uncertainties in: the consolidation

times under the PCMs, in the load and resistance of the PCM restraint, and how much movement might occur at each cycle if the load (assuming no movement) exceeds the resistance.

Every one of the above ingredient uncertainties could in-itself require a more detailed investigation. For instance, since information available on the McPac connector was limited, OneSubsea, the supplier of the connector, was engaged, and performed detailed local FE analyses of the connector, including factors that could affect the metal-to-metal contact seals under bending and pressure loads. This was then used to estimate the probability distribution of the bending moments on the restraint that might cause a leak due to loss of a metal-to-metal contact seal.

Combining all of the above in a probabilistic model, led to the conclusion that the most likely failure scenario (if failure occurs) would be that walking continues even after the soil under the PCMs is fully consolidated. The probability of this scenario, can be estimated much more simply, by comparing the maximum load that develops on an immobile constraint with the actual drained resistance provided by the PCMs, as is done in Figure 7.

Even if this "failure" scenario did develop, additional PCMs could be added before it is too late, or more weight could be added on top of the existing PCMs (to the extent that the design margins from the structural design of the PCMs themselves allow it). For this reason, a probability of "failure" of 2% was judged tolerable, since "failure" only means the need to take further action.

The matter of safety margins required to cover uncertainties for restraints to stop walking is a more general issue for the industry, for which no standardized industry approach is yet available. The uncertainties are mostly geotechnical (i.e. large compared to typical structural uncertainties), and these geotechnical uncertainties are compounded, as they occur on both the load- and resistance sides. If, despite these large uncertainties, a low failure probability is demanded, the required design margin will be large, resulting in large and expensive restraints. However, with suitable monitoring, and a contingency plan the consequences "failure" can be minimized, so that a higher probability of "failure" can be tolerated. Indeed, for such cases "restraint deficiency" is a better term than "failure". The safety margins for restraints to stop walking is one of the issues currently being addressed in the APT JIP led by Crondall Energy, Crondall Energy (2016).

Fabrication and Installation on a Live Flowline

Whereas Shell with support from Crondall Energy took the responsibility to ensure that the PCMs would indeed stop the walking without damaging the pipe or pushing it too deep into the soil before the PCMs close on it, Subcon took the responsibility for the detailed design and fabrication of the PCMs and logmats themselves. The detailed design of the PCMs was complicated by the need to ensure a suitable weight distribution within the PCM (to maximize clamping force) and the requirement for holes in the mattresses to reduce the time required for drainage to occur. Further, the PCM comprises two basic halves, with internal structural wires to tie the two halves together in the same way that the blocks of ordinary concrete mattresses are tied together. To ensure reliable clamping performance tight tolerances are required to control the gap between the two halves, and for the parts of the mold that form the clamping surface. Other complications included the design of suitable lifting points for fabrication, transportation and installation. As a result, fabrication required a very complex mold. The concrete was poured with the PCM upside down, and subsequently flipped over once curing had achieved a suitable strength. The final design also included markings to aid installation and allow measurement of embedment and any future movement, Figure 11. The mattresses fabrication took place at a temporary facility at Batangas in the Philippines, developed specifically for the project.

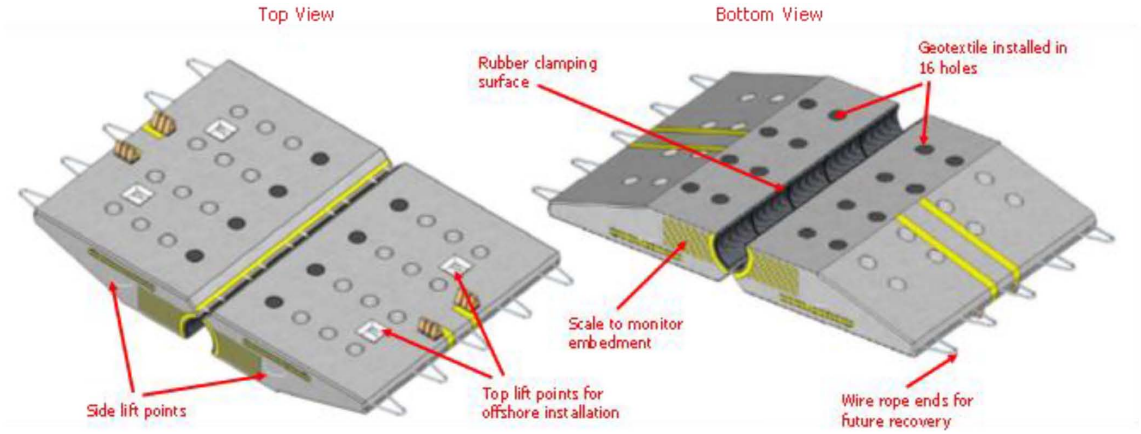

Figure 11—Final detailed PCM design, showing key installation and monitoring details

Installation of the PCMs was undertaken by DOF subsea from the Skandi Hawk. Some preparatory work was required prior to installation of the PCMs. Initially the surface of the pipe was cleaned to ensure that the axial friction generated between the clamp and the pipe was not compromised by any marine growth. At the target location, the pipe was typically embedded to between 30% and 40% of its diameter. To ensure that soil entrainment would not compromise the clamping operation, a plough was used to remove excessive material, and reduce the local embedment to 25% OD or less. The PCMs were transferred from the deck of the vessel to the seabed using a lifting frame, Figure 12

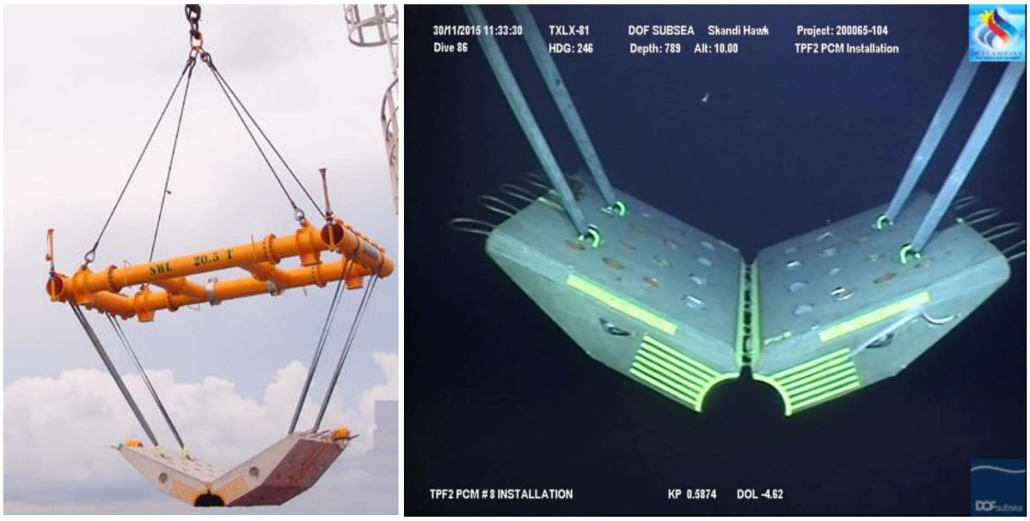

Figure 12—PCM deployment Offshore. (a) In-air. (b) Subsea

The rigging was designed to keep the PCM open at the optimum angle. This angle was a compromise between two competing effects; it was as large as practical to simplify contact with and grabbing of the pipe, but as small as practical to minimize the vertical load imposed on the pipe as the clamp closed (which may further embed the pipe prior to full clamping). Also, moving the lifting points on the PCM towards the hinge, instead of lifting it by the loops in the cables (as an ordinary mattress would be lifted) helps reduce the vertical load the PCM exerts on the pipe, before it closes on the pipe.

The PCMs were lowered to just above the seabed away from the pipe, and then maneuvered over the top of the pipe at a clearance of no more than 1 m to minimize any denting risk to the pipeline. (Simple energy balance calculations indicated that the dent from dropping the PCM from a height up to 1m would be tolerable.) Once over the pipeline, the PCM was slowly lowered down until contact was made with

the pipe. As contact became established, the PCM naturally closed around the pipe and self-aligned as the installation proceeded. It was found that, once partial clamping had been established, the PCM could be easily maneuvered along the axis of the pipe, to allow very accurate positioning of the PCM. Following installation of the PCMs, the log mats were deployed to the seabed in a similar manner and installed over the PCMs, Figure 13. Installation of 15 mattresses was completed in 10 days.

Figure 13—As-Installed PCM. (a) prior to installation of log-mat. (b) with log-mat installed

To minimize the axial displacements that must occur at the extremity of the PCM bank, it is desirable to install the PCMs over as short a distance as practical. However, it was not possible to install the PCMS as a continuous bank due to the presence of anodes (on every second pipe joint at this location) and the need to avoid the coating field joints. A maximum of 3 PCMs could be installed on a single 12.2m pipe joint, so the 15 PCMs were installed as 5 banks of 3, Figure 14. This resulted in a total length of coverage of about 60 m.

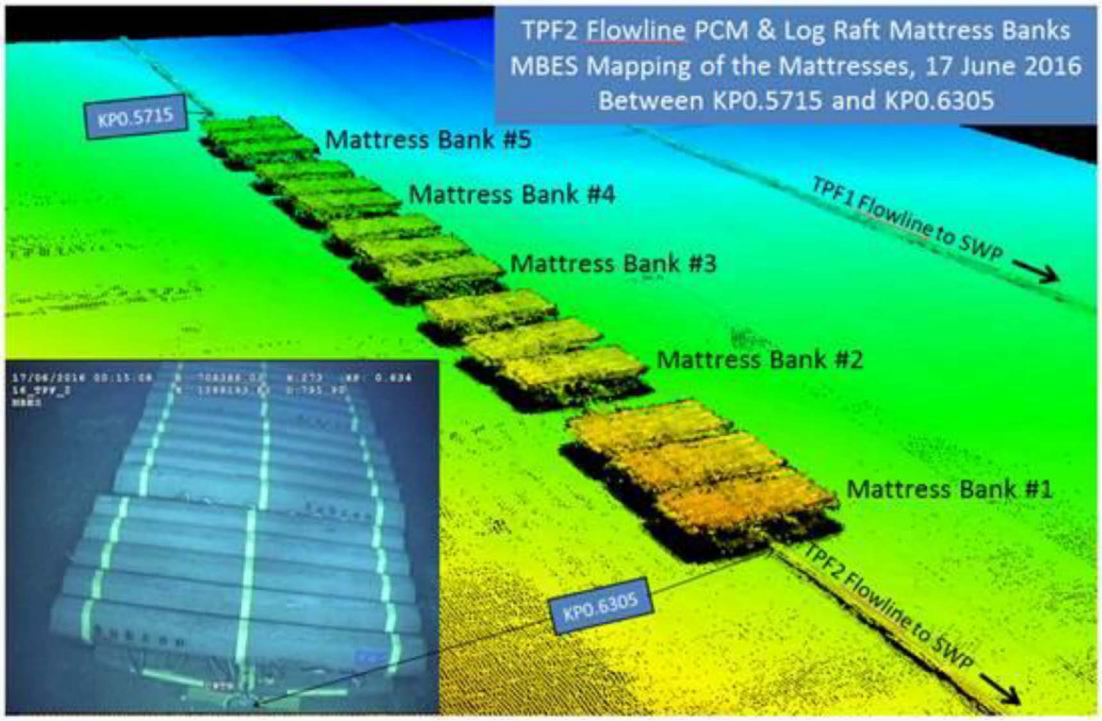

Figure 14—MBES overview image of the as-installed PCM banks.

Performance Monitoring

Checking to make sure that the PCMs do indeed stop the walking in this case is not just "nice to have" but essential, since the estimated probability that they fail to do so even after full consolidation is around 2% based on the estimated probability distributions of Figure 7. Such a high failure probability is tolerated, since it is always possible to add more PCMs if the ones deployed were not sufficient.

The first inspection in January 2016 did not reveal significant movement, from the installed flags, Figure 15. During the period from installation to the first inspection, 3 operating cycles occurred. Without the PCMs, these cycles would have produced about 8cm of walking displacements, which could have been detected by the flags. This suggests that even before full consolidation the PCMs already have sufficient capacity to stop the walking. Nevertheless, further monitoring is planned, in case small movements are occurring, which over the longer term might be detected by the flags.

Figure 15—Flags with ruler markings installed adjacent to PCMs to facilitate displacement measurement

Conclusions

The conditions that lead to inventing, fabricating and deploying the PCMs within a period of 12 months included:

- An axial restraint is needed to stop flowline walking.
- The optimal location for the restraint is away from the inlet (PLES). To restrain it at the PLES would require a much larger restraint capacity.
- No provision had been made for collar joints on which a clamp might be applied.
- It is preferred not to remove the coating. Therefore, the coating must withstand the clamping forces and shearing forces at the operating temperature of the pipeline.
- Rock dumping would require an expensive mobilization to a remote location.

For this the PCMs proved to be a simple, inexpensive, and effective solution. The possibility to use PCMs also can justify "wait and see" approach for new projects, where there is uncertainty about whether the flowline will walk, to avoid installation of unnecessary restraints. It is also always possible to add more PCMs, if necessary. This makes the large design margins that might otherwise be needed to cover uncertainty in load and resistance for the restraint unnecessary.

Acknowledgements

The development and successful installation of the PCMs involved vital contributions from a wide range of companies and individuals. Within Shell Projects and Technology, Giuseppe Pagliuca performed the transient flow simulations with Olga, using a model originally developed by Pek-San Ong, Jan van Bokhorst provided support in regard to the capacity of the 3-layer-PP coating to resist the PCM loads at the operating temperature of the pipeline, Leo de Mul reviewed thermoplastic materials for the clamping surface, Chris Kettle reviewed Cathodic Protection design and impact of electrolyte access restrictions due to the PCMs, Mike Coyne and Don Nelson performed the overall design and installability review. DOF Subsea, under the project leadership of Heng Yeu Tan, not only performed the installation, but also held the contract with Subcon for the detailed design and fabrication of the PCMs. Within Subcon John Holmes and Jonathon Curry were very effective and resourceful in overcoming the many technical and non-technical challenges involved. Finally, Fraser Bransby and Hongjie Zhou of Fugro AG contributed to the geotechnical analysis.

References

Atkins (2015) SAFEBUCK JIP: Safe design of pipelines with lateral buckling. *Design Guideline, SAFEBUCK III. 5087471/01/C* dated 15 January 2015.

Bruton, D., et al., (2010), "Lessons Learnt from Observing Walking of Pipelines with Lateral Buckles, Including New Driving Mechanisms and Updated Analysis Models," 2010 Offshore Technology Conference, Houston, Texas, 3-6 May 2010, Paper No. OTC 20750.

Carneiro, D., Rathbone, A., Soon, K.S., Viecelli, G. (2014) "Rate Dependent Soil Resistance in FE Analysis of Pipeline Walking," Proceedings of the ASME 2014 33rd International Conference on Ocean, Offshore and Arctic Engineering, June 8-13, San Francisco, California, USA, Paper No. OMAE2014-23521.

Carr, M., Sinclair, F., and Bruton, D., 2006, "Pipeline Walking - Understanding Field Layout Challenges, and Analytical Solutions Developed for the Safebuck JIP," Offshore Technology Conference, Houston Texas, USA, 1-4 May 2006, Paper No. OTC 17945.

Clark A.R. and Walker B.F. (1977). A proposed scheme for the classification and nomenclature for use in the engineering description of Middle Eastern sedimentary rocks. *Géotechnique* Vol. **27**, No.1, 93–99

Crondall Energy (2016). Anchoring Pipeline Technology – a new Joint Industry Project. *The APT JIP*.

Konuk, I. (1998) "Expansion of Pipelines under Cyclic Operational Conditions" *OMAE 1998*.

Peek, R. (2002) "Crawling of Pipelines under Cyclic Thermal Loading," *Shell Global Solutions International, Report No. OP 02-30011*, Reviewed by P.R. Paslay and W.T. Jones, Revised 4th January 2002. Released as unrestricted, September 2016.

Tornes, K., Jury, J., Ose, B., Thompson. (2000) "Axial Creeping of High Temperature Flowlines Caused by Soil Ratcheting", *OMAE* 2000.

White D.J., Westgate Z.J., Ballard J-C, de Brier C. & Bransby M.F. (2015). "Best practice geotechnical characterization and pipe-soil interaction analysis for HPHT flowline design". Proc. Offshore Technology Conference, Houston Paper OTC26032-MS.

White D.J., Campbell M.E., Boylan N.P. & Bransby M.F. (2012). A new framework for axial pipe-soil interaction illustrated by shear box tests on carbonate soils. Proc. Int. Conf. on Offshore Site Investigation and Geotechnics. SUT, London. 379–387